



Published in final edited form as:

Cell Rep. 2014 October 09; 9(1): 366–377. doi:10.1016/j.celrep.2014.08.057.

Central Ceramide-Induced Hypothalamic Lipotoxicity and ER Stress Regulate Energy Balance

Cristina Contreras^{1,2,10}, **Ismael González-García**^{1,2,10}, **Noelia Martínez-Sánchez**^{1,2}, **Patricia Seoane-Collazo**^{1,2}, **Jordi Jacas**^{2,3}, **Donald A. Morgan**⁴, **Dolors Serra**^{2,5}, **Rosalía Gallego**⁶, **Francisco Gonzalez**^{7,8}, **Núria Casals**^{2,3}, **Rubén Nogueiras**^{1,2}, **Kamal Rahmouni**^{4,9}, **Carlos Diéguez**^{1,2}, and **Miguel López**^{1,2,*}

¹Department of Physiology, CIMUS, University of Santiago de Compostela-Instituto de Investigación Sanitaria, 15782 Santiago de Compostela, Spain

²CIBER Fisiopatología de la Obesidad y Nutrición (CIBERObn), 15706 Santiago de Compostela, Spain

³Basic Sciences Department, Faculty of Medicine and Health Sciences, Universitat Internacional de Catalunya, Sant Cugat del Vallés, 08195 Barcelona, Spain

⁴Department of Pharmacology, University of Iowa, Iowa City, IA 52242, USA

⁵Department of Biochemistry and Molecular Biology, School of Pharmacy, Institut de Biomedicina (IBUB), Universitat de Barcelona, 08028 Barcelona, Spain

⁶Department of Morphological Sciences, School of Medicine, University of Santiago de Compostela, 15782 Santiago de Compostela, Spain

⁷Department of Surgery, CIMUS, University of Santiago de Compostela-Instituto de Investigación Sanitaria, 15782 Santiago de Compostela, Spain

⁸Service of Ophthalmology, Complejo Hospitalario Universitario de Santiago de Compostela, 15706 Santiago de Compostela, Spain

⁹Department of Internal Medicine, University of Iowa, Iowa City, IA 52242, USA

SUMMARY

This is an open access article under the CC BY-NC-ND license (<http://creativecommons.org/licenses/by-nc-nd/3.0/>).

*Correspondence: m.lopez@usc.es.

¹⁰Co-first author

SUPPLEMENTAL INFORMATION

Supplemental Information includes Supplemental Experimental Procedures, two figures, and three tables and can be found with this article online at <http://dx.doi.org/10.1016/j.celrep.2014.08.057>.

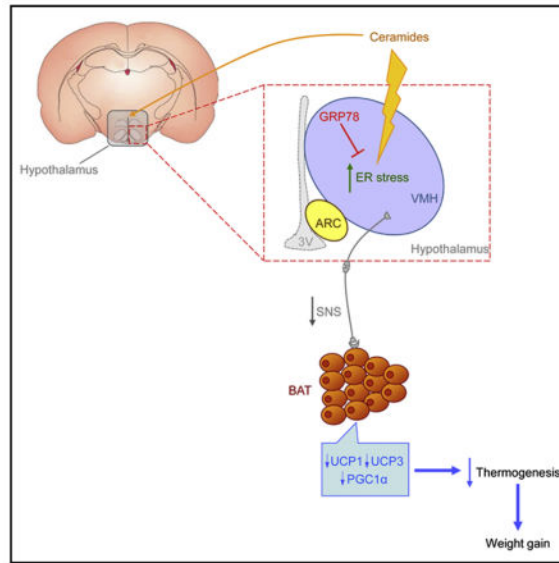
AUTHOR CONTRIBUTIONS

C.C., I.G.-G., N.M.-S., and P.S.-C. performed the in vivo experiments (implantation of intracerebroventricular cannulae and central treatments, stereotaxic protocols, GTTs, and ITTs) and analytical methods (serum analyses, quantitative PCR, and western blotting) and collected and analyzed the data. J.J., D.S., and N.C. performed the ceramide quantification. D.A.M. and K.R. performed and analyzed the sympathetic nerve activity recording studies. R.G. performed the immunohistochemistry. C.C., I.G.-G., R.N., K.R., C.D., and M.L. designed the experiments. C.C., I.G.-G., F.G., R.N., K.R., C.D., and M.L. discussed the manuscript. C.C. and M.L. made the figures. M.L. coordinated and directed the project, developed the hypothesis, and wrote the manuscript.

Hypothalamic endoplasmic reticulum (ER) stress is a key mechanism leading to obesity. Here, we demonstrate that ceramides induce lipotoxicity and hypothalamic ER stress, leading to sympathetic inhibition, reduced brown adipose tissue (BAT) thermogenesis, and weight gain. Genetic overexpression of the chaperone GRP78/BiP (glucose-regulated protein 78 kDa/binding immunoglobulin protein) in the ventromedial nucleus of the hypothalamus (VMH) abolishes ceramide action by reducing hypothalamic ER stress and increasing BAT thermogenesis, which leads to weight loss and improved glucose homeostasis. The pathophysiological relevance of this mechanism is demonstrated in obese Zucker rats, which show increased hypothalamic ceramide levels and ER stress. Overexpression of GRP78 in the VMH of these animals reduced body weight by increasing BAT thermogenesis as well as decreasing leptin and insulin resistance and hepatic steatosis. Overall, these data identify a triangulated signaling network involving central ceramides, hypothalamic lipotoxicity/ER stress, and BAT thermogenesis as a pathophysiological mechanism of obesity.

In Brief

The brain senses lipids, such as fatty acids, and modifies energy metabolism accordingly. However, it is unclear whether other lipid species may be involved. Contreras et al. now demonstrate that ceramides regulate energy balance through the induction of hypothalamic lipotoxicity and modulation of endoplasmic reticulum functionality. This leads to changes in sympathetic tone and brown adipose tissue (BAT)-induced thermogenesis, impacting body weight.



INTRODUCTION

Obesity and its related metabolic disorders are increasing at a rate that is considered of epidemic proportions in Western and developing countries. The increasing prevalence of obesity is likely due to a combination of genetic predisposition as well as evolutionary, social, and environmental factors (Gregor and Hotamisligil, 2011; Ramachandrapa and Farooqi, 2011; Speakman and O’Rahilly, 2012). Data gleaned over the last few years have

uncovered the interaction between peripheral signals and brain targets provided by different neuropeptides and neurotransmitters (Lam et al., 2005; Luquet and Magnan, 2009; Yeo and Heisler, 2012). However, despite initial hope, this knowledge failed to provide a much-needed antiobesity drug (Finan et al., 2012; Dietrich and Horvath, 2012; Malik et al., 2013). It is generally recognized that to progress in this area it is crucial to discover the basic molecular mechanisms regulating energy homeostasis. Taking into account that almost all signaling proteins used by cells to communicate with its environment are assembled in the endoplasmic reticulum (ER) (Schröder and Kaufman, 2005; Ron and Walter, 2007; Gregor and Hotamisligil, 2011; Fu et al., 2012), studies addressing the molecular mechanisms involved in ER stress functions have started to reveal the molecular mechanisms involved in complex diseases.

The ER is a sophisticated luminal network in which protein synthesis, maturation, folding, and transport take place (Schröder and Kaufman, 2005; Marciniak and Ron, 2006; Ron and Walter, 2007; Gregor and Hotamisligil, 2011; Fu et al., 2012). The term ER stress refers to the alterations of the protein-folding functionality of the ER, which activates a complex signaling network termed the unfolded protein response (UPR), leading to coordinated transcriptional events promoting attenuation of protein synthesis, upregulation of ER-folding machinery (a type of proteins called chaperones), and degradation of irreversibly misfolded proteins (Schröder and Kaufman, 2005; Marciniak and Ron, 2006; Ron and Walter, 2007; Martínez de Morentin and López, 2010; Fu et al., 2012). Previous studies have demonstrated that ER stress and activation of UPR pathways play a major role promoting obesity-induced insulin resistance in peripheral tissues. For example, inflammation, free lipid accumulation, and hyperglycemia in pancreatic β cells and liver elicit activation of the UPR, leading to decreased insulin expression and inhibition of insulin signaling (Ozcan et al., 2004, 2006; Lipson et al., 2006; Kammoun et al., 2009; Fu et al., 2012). Current evidence also indicates that obesity and overnutrition-induced inflammation causes ER stress in the hypothalamus, inducing insulin and leptin resistance and, ultimately, weight gain (Zhang et al., 2008; Hosoi et al., 2008; Ozcan et al., 2009; Won et al., 2009; Ropelle et al., 2010; Schneeberger et al., 2013). Notably, these studies also demonstrate that pharmacological interventions that improve protein folding (i.e., chemical chaperones) recover leptin and insulin signaling, normalizing body weight (Zhang et al., 2008; Hosoi et al., 2008; Ozcan et al., 2009; Won et al., 2009; Schneeberger et al., 2013).

A current idea gaining credibility is that adipose stores in some obese individuals become saturated and lipotoxic fat metabolites spill over into tissues not suited for lipid storage (Virtue and Vidal-Puig, 2010; Martínez de Morentin et al., 2010). Thus, accumulation of reactive lipid species, such as diacylglycerol, free fatty acids, free cholesterol, and ceramides, is a pathogenic mechanism of insulin resistance, type 2 diabetes, and liver and cardiovascular disease. In peripheral tissues, such as β cells, skeletal muscle, liver, and heart, this process, known as lipotoxicity, occurs through inflammation and ER stress (Unger, 2002; Virtue and Vidal-Puig, 2008; Symons and Abel, 2013). However, despite this evidence, whether (1) lipotoxicity may happen in the hypothalamus and, more specifically, whether (2) ceramide-induced lipotoxicity may induce hypothalamic ER stress or (3) this mechanism is of relevance for obesity is currently unknown. Therefore, the aims of this study were first to determine whether central ceramides elicit ER stress in the hypothalamus,

and second to investigate whether that action accounts for the changes in energy balance associated with obesity.

RESULTS

Central Ceramide Treatment Induced Hypothalamic ER Stress and Body Weight Gain through Sympathetic Inhibition of BAT

Central treatment of C6 ceramide, a cell-penetrating ceramide that is partially converted to long-chain ceramides inside the cell (Mitoma et al., 1998; Gao et al., 2011; Ramírez et al., 2013), increased the concentration of C16 ceramide in the mediobasal hypothalamus (MBH), confirming the efficiency of the treatment (Figure 1A). This effect was associated with increased ER stress, as demonstrated by the increased protein concentration of the UPR, such as GRP78/BiP (glucose-regulated protein 78 kDa/binding immunoglobulin protein), pIRE1 (phosphorylated inositol requiring enzyme 1), pPERK (phosphorylated PKR-like ER kinase), peIF2 α (phosphorylated eukaryotic initiation factor 2 α), ATF6 α (activating transcription factor 6 alpha), and CHOP (C/EBP homologous protein) (Schröder and Kaufman, 2005; Marciniak and Ron, 2006; Ron and Walter, 2007; Martínez de Morentin and López, 2010; Fu et al., 2012) in the MBH (Figure 1B). Of note, central administration of ceramide induced a marked feeding-independent weight gain (Figure 1C), which was associated with decreased mRNA levels of thermogenic markers in BAT, such as uncoupling proteins 1 and 3 (UCP1 and UCP3), peroxisome-proliferator-activated receptor-gamma coactivator 1 alpha (PGC1 α , but not PGC1 β), and fatty acid-binding protein 3 (FABP3) (Figure 1D). This was confirmed at the protein level as indicated by the reduced UCP1 protein concentration in BAT (Figure 1E). In keeping with the decreased expression of thermogenic markers, central ceramide-treated rats displayed lower body temperature (Figure 1F). Moreover, central administration of ceramide reduced BAT sympathetic nerve traffic recorded directly by microneurography (Figures 1G–1H).

GRP78 in the Ventromedial Nucleus of the Hypothalamus Reversed the Central Ceramide Effect on Body Weight and BAT Thermogenesis

To assess the role of ER stress on ceramide-induced actions on energy balance, we targeted GRP78, an ER chaperone that facilitates the proper protein folding acting upstream of the UPR (Schröder and Kaufman, 2005; Marciniak and Ron, 2006; Ron and Walter, 2007; Martínez de Morentin and López, 2010; Fu et al., 2012; Cnop et al., 2012). Thus, an adenovirus encoding GRP78 wild-type (GRP78 WT) together with GFP or control adenovirus expressing GFP alone was injected first into the ventromedial nucleus of the hypothalamus (VMH), a key site modulating BAT (López et al., 2010; Martínez de Morentin et al., 2012, 2014; Whittle et al., 2012; Beiroa et al., 2014). Infection efficiency in the VMH was assessed by expression of GFP (Figure 2A) and an increased concentration of GRP78 in the VMH (Figure 2B). The specificity of the VMH dissections was 92.08% ($p < 0.001$) when using pro-opiomelanocortin (POMC) as a marker of “contamination” from the neighboring arcuate nucleus of the hypothalamus (ARC). GRP78 adenovirus elicited a marked decrease in four out the five proteins of the UPR tested in the VMH (Figure 2B), without changes in ceramide levels (Figure 2C), indicating that GRP78 was acting downstream of ceramides. Of note, central ceramide treatment increased the expression of

inflammatory markers in the hypothalamus such as interleukin 6 (IL6, but not IL1 β), phospho-IKK α/β (pIKK α/β), and tumor necrosis factor alpha (TNF α), which is indicative of lipotoxicity (Figure S1A). Remarkably, these effects of ceramide were not affected by GRP78 adenovirus (Figure S1A), confirming previous evidence that inflammation is upstream to ER stress in the hypothalamus (Zhang et al., 2008). Moreover, we found that administration of GRP78 adenovirus into the VMH reversed ceramide-induced weight gain without any change in food intake (Figure 2D). GRP78 WT adenovirus did not affect body weight or feeding in vehicle-treated rats (Figures S1B and S1C). Central ceramide promoted an increase in the weight of gonadal and inguinal white adipose tissue pads (gWAT and iWAT, respectively), an effect that was reversed by GRP78 adenovirus into the VMH (Figure 2E). In association with the increased adiposity, ceramide-treated rats showed a tendency for higher circulating leptin and triacylglyceride (TAG) levels that was partially reversed by GRP78 WT adenovirus (Table S1). The central ceramide-mediated decrease in UCP1 protein levels in the BAT (Figure 2F), BAT temperature (Figure 2G), and body temperature (Figure 2H) were also blunted by administration of GRP78 adenovirus in the VMH. Overall, these changes indicated that the central ceramide-induced ER stress effectively modulated BAT thermogenesis.

Next, GRP78 WT adenoviruses were injected within the ARC (Figure S1D), where they promoted an increase of the concentration of GRP78, which was concomitant to decreased levels of ER stress markers (Figure S1E). The specificity of the ARC dissections was 83.48% ($p < 0.001$), when using steroidogenic factor-1 (SF1) as a marker of contamination from the adjacent VMH. When given into the ARC, GRP78 WT adenovirus did not affect body weight (Figure S1F), feeding (Figure S1G), or BAT UCP1 protein content (Figure S1H).

GRP78 in the VMH Reversed the Central Ceramide Effect on Insulin Resistance

Given the effects of central ceramide administration on body weight and BAT thermogenesis, we next evaluated its impact on glucose homeostasis and insulin action. Our data showed that central ceramide did not impact glucose tolerance (Figure 3A) but impaired insulin sensitivity, which was reversed by GRP78 adenovirus in the VMH (Figures 3B and 3C).

Inactivation of GRP78 in the VMH Induced ER Stress and Weight Gain and Decreased UCP1 in BAT

Having shown that GRP78 overexpression in the VMH inhibited central ceramide's anabolic actions, we next investigated whether GRP78 inactivation in the same hypothalamic nucleus would have the opposite effect on body weight and BAT markers. For this, we treated rats with an adenovirus harboring a dominant-negative isoform of GRP78 (GRP78 DN) (Shen et al., 2002) in the VMH or the ARC. Infection efficiency was assessed by expression of GFP (similarly to Figures 2A and S1D for GRP78 WT) and increased concentration of GRP78 in the VMH or ARC, since GRP78 DN isoform was most likely recognized by GRP78 antibody (Figures 4A and S2A). Our data demonstrated that stereotaxic delivery of GRP78 DN induced a significant UPR activation in the VMH (Figure 4A), which accounts for increased ER stress, feeding-independent weight gain (Figures 4B and 4C), and decreased

UCP1 concentration in BAT (Figure 4D). On the other hand, despite ER stress induction in the ARC (Figure S2A), GRP78 DN adenovirus did not impact body weight (Figure S2B), food intake (Figure S2C), or UCP1 protein levels in BAT (Figure S2D).

GRP78 in the VMH Reversed Ceramide-Induced ER Stress in Obese Zucker Rats

To elucidate the contribution of ceramide-induced ER stress in the context of obesity, we used obese Zucker rats (OZR). Our data showed increased concentration of ceramide C16 and C18 in the MBH of OZR when compared to lean Zucker rats (LZR) (Figure 5A). In addition, UPR response was increased in the VMH of OZR (Figure 5B), indicating ER stress. Next, we evaluated the effect of GRP78 overexpression in the VMH of LZR and OZR. Our results indicate that stereotaxic injection of GRP78 WT adenovirus into the VMH induced feeding-independent weight loss in OZR, but not in LZR (Figures 5C and 5D), and ameliorated hypothalamic ER stress (Figure 5E) without changes in hypothalamic ceramide levels (Figures 5F and 5G).

GRP78 in the VMH Increased BAT Thermogenesis and Improved the Metabolic Profile of Obese Zucker Rats

Next, we investigated the effect of GRP78 WT adenovirus on thermogenesis. Our data showed that reversion of hypothalamic ER stress with GRP78 WT induced a marked increase in UCP1 protein levels in BAT (Figure 6A), as well as increased BAT (Figure 6C) and core temperature (Figure 6E) in OZR, indicating increased thermogenesis. These effects were associated with an improvement in the metabolic phenotype of OZR, as demonstrated by decreased hepatic steatosis (Figure 6G) associated with reduced levels of acetyl-coenzyme A carboxylase alpha (ACC α ; data not shown) and iWAT weight (Figure 6I) and reduced circulating cholesterol and TAG levels (Table S2). Of note, no changes were detected in LZR rats treated with the GRP78 WT adenovirus (Figures 6A, 6B, 6D, 6F, and 6H).

GRP78 in the VMH Improves Leptin Signaling and Insulin Resistance in Obese Zucker Rats

Administration of GRP78 WT adenovirus into the VMH did not affect the protein levels of pSTAT3 (phosphorylated signal transducer and activator of transcription 3), pPI3K (phosphorylated phosphatidylinositide 3-kinase), phosphorylated AKT (pAKT), and SOCS3 (suppressor of cytokine signaling 3) in the VMH of LZR rats (Figure 7A). GRP78 WT adenoviruses induced significantly the concentration of pSTAT3, pPI3K, and pAKT in the VMH of OZR, whereas SOCS3 levels were reduced (Figure 7B).

Administration of GRP78 WT adenovirus into the VMH did not affect glucose tolerance in either LZR or OZR, although they reduced insulin circulating levels as early as 30 min after glucose administration in OZR (Figures 7C and 7D). On the other hand, GRP78 WT adenoviruses tended to increase insulin sensitivity in LZR (Figure 7E). Notably, this effect was more pronounced in OZR, where a significant improvement in insulin resistance was found (Figure 7F). In keeping with these data, GRP78 WT adenovirus increased the levels of pAKT in the muscle (Figure 7H) and the levels of pPI3K and pAKT in the liver (Figure 7J) of OZR. No significant changes were observed in LZR (Figures 7G and 7I). Overall, this

evidence demonstrates that GRP78 WT into the VMH treatment improves insulin sensitivity in OZR.

DISCUSSION

This study identifies a physiological link among ceramides, hypothalamic ER stress, and the modulation of energy balance. Specifically, we show that ceramide-induced hypothalamic lipotoxicity and ER stress elicits decreased sympathetic tone to BAT, which leads to decreased thermogenesis and feeding-independent weight gain. In addition, we show that genetic modulation of the ceramide-induced ER stress pathway in a specific hypothalamic nucleus, the VMH, modulates energy balance by influencing BAT thermogenesis in a sympathetic nervous system (SNS)-mediated manner and insulin sensitivity, as well as by promoting an overall improvement of the metabolic phenotype of leptin and insulin resistant obese Zucker rats.

Ceramides comprise a family of simple sphingolipids generated from fatty acid and sphingosine (Bikman and Summers, 2011; Chavez and Summers, 2012). Although ceramides are present at low levels within biological membranes, they make important contributions to cell membrane structure. In addition, ceramides exert diverse regulatory effects on cell-signaling pathways that mediate growth, proliferation, motility, adhesion, differentiation, senescence, and apoptosis (Holland and Summers, 2008; Hannun and Obeid, 2008; Cowart, 2009). Increased ceramide production can lead to ER stress, a mechanism underlying insulin resistance and liver diseases (Kahn et al., 2006; Holland and Summers, 2008; Bikman and Summers, 2011; Chavez and Summers, 2012). In keeping with this, systemic pharmacological inhibition or global genetic ablation of de novo synthesis of ceramides improves insulin sensitivity and glucose homeostasis (Summers et al., 1998; Yang et al., 2009) and protects against glucocorticoid-, saturated fat-, and obesity-induced insulin resistance (Holland et al., 2007). Current evidence indicates that brain ceramide levels are increased during high-fat diet-induced obesity (Borg et al., 2012) and in streptozotocin-induced diabetic rats (Car et al., 2012). Also, hypothalamic ceramide levels regulated by carnitine palmitoyltransferase 1c (CPT1c, a specific isoform located in the ER), mediate the orexigenic effect of ghrelin (Ramírez et al., 2013). Finally, current evidence has related hippocampal ceramides with impaired energy balance and weight gain (Picard et al., 2014). However, despite of this evidence, no data have linked hypothalamic ceramide-induced lipotoxicity with ER stress and energy homeostasis. Therefore, we hypothesized that positive energy balance in obesity might be mediated by specific alterations in hypothalamic ceramide levels and ER stress.

Our data demonstrate that central administration of C6 ceramide (which acts as a long-chain ceramide precursor) increases the C16 ceramide concentration in the ventromedial hypothalamus. Of note, this effect was associated with feeding-independent weight gain, hypothalamic inflammation (leading to lipotoxicity), and increased concentration of UPR proteins (a functional indicator of elevated ER stress), alongside with a decrease in SNS firing and thermogenic capacity of BAT. To determine the physiological relevance of these observations, we investigated whether selective modulation of hypothalamic UPR (and then ER stress) was sufficient to overrule central ceramide's effects in vivo. For this purpose, we

focused on the chaperone GRP78 (also called BiP). GRP78 is the most abundant ER-resident chaperone that can prevent accumulation of unfolded/misfolded proteins within the ER (Schröder and Kaufman, 2005; Marciniak and Ron, 2006; Ron and Walter, 2007; Martínez de Morentin and López, 2010; Fu et al., 2012; Cnop et al., 2012). Our data showed that chronic intracerebroventricular (ICV) ceramide administration increased GRP78 protein concentration in the MBH, as an adaptive response to ameliorate ER stress. To test this possibility, we treated rats with adenoviral particles overexpressing GRP78 specifically within the VMH, which is known to control BAT thermogenesis through the SNS (Cannon and Nedergaard, 2004; López et al., 2010; Martínez de Morentin et al., 2012, 2014; Whittle et al., 2012; Beiroa et al., 2014). We show that GRP78 overexpression in the VMH reduces ER stress and reverses the anabolic effects of central ceramide administration by promoting weight loss (independently of food intake), increasing UCP1 protein content in BAT, and thermogenesis. Conversely, inactivation of GRP78 (by adenoviral-driven expression of DN isoforms) within the VMH promotes ER stress and increases body weight in a feeding-independent manner, in association with decreased UCP1 expression in BAT. Remarkably, no effect on body weight or BAT thermogenesis was detected when GRP78 was targeted (by using either WT or DN adenoviruses) in the neighboring ARC, which has been primarily involved in the regulation of feeding, rather than energy expenditure (Yeo and Heisler, 2012; Williams and Elmquist, 2012; López et al., 2013). Overall, these data suggest that ceramides and GRP78 regulate energy balance in an anatomical-specific pattern. In keeping with this concept, ceramide-induced insulin resistance is also improved when GRP78 was overexpressed within the VMH that is also recognized as a key site modulating glucose homeostasis (McCrimmon et al., 2006, 2008). Although, classically, the VMH is considered to be a regulator of feeding control (“the satiety center”), our data reinforce recent proofs revealing a more complex physiological role. These data support the idea that the VMH is a fundamental brain area in the regulation of thermogenesis and energy balance, integrating peripheral signaling (i.e., thyroid hormones, bone morphogenetic protein 8b, estradiol, and glucagon like peptide-1) and metabolite sensing (i.e., fatty acids and ceramides) with cellular energy sensors (i.e., AMP-activated protein kinase) (McCrimmon et al., 2006, 2008; López et al., 2008, 2010; Whittle et al., 2012; Martínez de Morentin et al., 2014; Beiroa et al., 2014) and now with cellular machinery, namely ER stress and UPR.

A typical problem associated with malfunction of the central mechanism governing energy balance is the development of resistance to peripheral signals, such as insulin and leptin (Caro et al., 1996; Howard et al., 2004). Current evidence has demonstrated that one of the pathological mechanisms of leptin resistance is hypothalamic ER stress (Zhang et al., 2008; Hosoi et al., 2008; Ozcan et al., 2009; Won et al., 2009; Ropelle et al., 2010; Schneeberger et al., 2013). Remarkably, these studies demonstrate that pharmacological interventions that improve protein folding (i.e., chemical chaperones) recover leptin and insulin signaling, normalizing body weight (Zhang et al., 2008; Hosoi et al., 2008; Ozcan et al., 2009; Won et al., 2009; Schneeberger et al., 2013). Nevertheless, most of the current evidence has been related to the ARC (i.e., melanocortin neurons) and feeding. Here, we focused on the pathophysiological relevance of ER stress in the VMH using a well-established model of leptin resistance, the OZR, which presents a defective leptin receptor signaling (Phillips et al., 1996). We observed increased hypothalamic ceramide levels in Zucker rats, associated

with increased UPR and ER stress in the VMH. Next, we stereotaxically treated OZR with an adenovirus harboring GRP78 into the VMH. That paradigm recapitulated the previous data, with GRP78 promoting an amelioration of the hypothalamic ER stress associated with marked negative energy balance in OZR, leading to increased BAT thermogenesis, and improved metabolic profile as indicated by the weight loss and the increased leptin signaling and insulin sensitivity, as well as reduced liver steatosis and circulating lipid levels. Notably, these effects were totally independent of feeding behavior, as food intake remained unchanged after the adenoviral treatment. Overall, these data indicate that modulation of ER stress in the VMH ameliorates obesity in an extreme model of leptin resistance, which is a condition in human obesity (Caro et al., 1996; Howard et al., 2004).

Conventionally, the toxic effects of the accumulation of lipids, such as ceramides, have been located in peripheral tissues, such as pancreatic β cells, and liver, heart, and skeletal muscle, where they have been linked with inflammation and the pathophysiology of insulin resistance, type 2 diabetes, liver disease, atherosclerosis, and cardiovascular disease (Unger, 2002; Virtue and Vidal-Puig, 2008; Symons and Abel, 2013). Of note, lipotoxicity can also occur in the CNS, as observed in certain neurodegenerative disorders (i.e., polyglutamine diseases, Parkinson's disease, and amyotrophic lateral sclerosis) (Ilieva et al., 2007). However, one key question that remained to be addressed relates the status of lipid metabolism and whether accumulation of specific lipid species occurs in the hypothalamus, leading to lipotoxicity, which might have deleterious effects on energy homeostasis. Here, we present evidence demonstrating that ceramides play a key role within the hypothalamus to modulate energy balance through induction of lipotoxicity ER stress and modulation of BAT function. Thus, our data provide an alternative hypothalamic-centered paradigm showing that amelioration of central ER stress leads to a marked improvement in weight gain in a genetic model of obesity. Overall, these data identify a network involving central ceramides, hypothalamic lipotoxicity, ER stress, and VMH-regulated BAT thermogenesis as a pathophysiological mechanism promoting obesity and a promising target for therapeutic intervention.

EXPERIMENTAL PROCEDURES

Animals

Male Sprague-Dawley rats (200–250 g; Animalario General University of Santiago de Compostela (USC), Santiago de Compostela, Spain and Charles River Laboratories) and obese Zucker rats (OZR; fa/fa; 300–350 g) and their controls, LZR (fa/–; 250–300 g), both provided by Charles River, were used for the experiments. All animals were housed on a 12 hr light (8:00 to 20:00), 12 hr dark cycle, in a temperature- and humidity-controlled room. The animals were allowed free access to standard laboratory pellets of rat chow and tap water. In all the experimental settings, animals and their food were weighed daily at the beginning of the light phase. The experiments were performed in agreement with the International Law on Animal Experimentation and were approved by the USC Local Ethical Committee, the Xunta de Galicia (Project ID 15010/14/006), and the University of Iowa Institutional Animal Care and Use Committee.

Implantation of Intracerebroventricular Cannulae and Central Treatments

Chronic ICV cannulae were implanted under ketaminexylazine anesthesia (50 mg/kg, intraperitoneal), as described previously, and correct positioning in the lateral ventricle was confirmed by postmortem histological examination (López et al., 2008, 2010; Whittle et al., 2012; Martínez de Morentin et al., 2014). A catheter tube was connected from the brain infusion cannulae to an osmotic minipump flow moderator (model 2001; Alzet). The minipump was inserted in a subcutaneous pocket on the dorsal surface of the animal, created using blunt dissection. The incision was closed with surgical sutures. The rats were then infused with C6 ceramide (N-hexanoyl-D-sphingosine; 1.25 mg/ml dissolved in saline containing one-third DMSO; Sigma-Aldrich) or vehicle (saline containing one-third DMSO; control rats) for 5 days. The selection of these doses was based on previous reports (Ramírez et al., 2013). The animals were caged individually and used for experimentation 5–7 days later. During this postoperative recovery period, the rats became accustomed to the handling procedure under nonstressful conditions.

Stereotaxic Microinjection of Adenoviral Expression Vectors

Rats were placed in a stereotaxic frame (David Kopf Instruments) under ketamine-xylazine anesthesia. The VMH and ARC were targeted bilaterally using a 25G needle (Hamilton). The injections were directed to the following stereotaxic coordinates: (1) for the VMH, 2.4/3.2 mm posterior to the bregma (two injections were performed in each VMH), ± 0.6 mm lateral to midline and 10.1 mm ventral; and (2) for the ARC, 2.8 posterior to bregma, ± 0.3 mm lateral to midline and 10.2 mm ventral, as previously reported (López et al., 2008; López et al., 2010; Whittle et al., 2012; Martínez de Morentin et al., 2014; Beiroa et al., 2014). Adenoviral vectors (Viraquest) containing GFP (used as control), GRP78 WT (at 10^{12} particles/ml), GRP78 DN (dominant-negative, at 10^8 particles/ml) (Hendershot et al., 1995) were delivered at a rate of 200 nl/min for 5 min (1 μ l/injection site) as previously reported (López et al., 2008, 2010; Whittle et al., 2012; Martínez de Morentin et al., 2014; Beiroa et al., 2014). Animals were treated for 6–9 days.

Glucose and Insulin Tolerance Tests

Seven days after stereotaxic surgery, blood glucose levels were measured at 0, 15, 30, and 60 min after glucose or insulin administration with a glucometer (Accucheck, Roche) after an intraperitoneal injection of 0.75 U/kg insulin (Actrapid, Novonordisk) for insulin tolerance test (ITT) or 2 mg/g D-glucose (Sigma-Aldrich) administered orally via gavage for glucose tolerance test (GTT) (Beiroa et al., 2013). In this case, the animals were fasted overnight. To assay insulin sensitivity, insulin (100 U/ml; Actrapid, Novonordisk) was injected in the portal vein. Thirty seconds after the insulin injection, the liver was removed, and 90 s later the gastrocnemius muscle was extracted. All samples were immediately homogenized on ice.

Ceramide Quantification

Ceramides were extracted and analyzed via an liquid chromatography-electrospray ionization/multistage mass spectrometry system (API 3000 PE Sciex; Spectralab Scientific) in positive ionization as formerly described (Ramírez et al., 2013). Concentrations were

measured by multiple reaction monitoring experiments using N-heptadecanoyl-D-erythro-sphingosine (C17- ceramide) as an internal standard (50 ng/ml). The method was linear over the range from 2 to 600 ng/ml using as patrons N-palmitoyl-D-erythro-sphingosine (C16 ceramide) and N-stearoyl-D-erythro-sphingosine (C18 ceramide; Avanti Polar Lipids).

Sample Processing and Analytical Methods

Sample processing, serum analyses, temperature measurements, sympathetic nerve activity (SNA) recording, real-time quantitative PCR, western blotting, and immunohistochemistry were performed as described previously (López et al., 2008, 2010; Whittle et al., 2012; Martínez de Morentin et al., 2012, 2014; Seoane-Collazo et al., 2014; Beiroa et al., 2014) (see the Supplemental Experimental Procedures for detailed protocols).

Statistical Analysis

Data are expressed as mean \pm SEM. mRNA, and protein data were expressed in relation (%) to control (vehicle or GFP-treated) rats. SNA was expressed as a percent change from baseline. Statistical significance was determined by t-Student when two groups were compared or ANOVA and post hoc two-tailed Bonferroni test when more than two groups were compared. $p < 0.05$ was considered significant.

Supplementary Material

Refer to Web version on PubMed Central for supplementary material.

Acknowledgments

The research leading to these results has received funding from the European Community's Seventh Framework Programme (FP7/2007–2013) under grant agreement no. 281854, the OberStress European Research Council Project (M.L.), and 245009, the Neurofast project (R.N., C.D., and M.L.), Xunta de Galicia (F.G., 10PXIB208126PR; R.N., EM 2012/039 and 2012-CP069; M.L., 2012-CP070), Instituto de Salud Carlos III (ISCIII; M.L., PI12/01814), MINECO cofunded by the FEDER Program of EU (F.G., BFU-2010-14968; D.S., SAF2011-30520-C02-01; R.N., BFU2012-35255; N.C., SAF2011-30520-C02-02; C.D., BFU2011-29102), and the NIH (K.R.: HL084207). I.G.-G. is a recipient of a fellowship from Ministerio de Educación, Cultura y Deporte (FPU12/01827). CIBER de Fisiopatología de la Obesidad y Nutrición is an initiative of ISCIII. The funders had no role in study design, data collection and analysis, decision to publish, or preparation of the manuscript.

References

- Beiroa D, Romero-Picó A, Langa C, Bernabeu C, López M, López-Novoa JM, Nogueiras R, Diéguez C. Heterozygous deficiency of endoglin decreases insulin and hepatic triglyceride levels during high fat diet. *PLoS ONE*. 2013; 8:e54591. [PubMed: 23336009]
- Beiroa, D.; Imbernon, M.; Gallego, R.; Senra, A.; Herranz, D.; Villaroya, F.; Serrano, M.; Fernø, J.; Salvador, J.; Escalada, J., et al. GLP-1 Agonism Stimulates Brown Adipose Tissue Thermogenesis and Browning Through Hypothalamic AMPK. *Diabetes*. 2014. <http://dx.doi.org/10.2337/db14-0302>
- Bikman BT, Summers SA. Ceramides as modulators of cellular and whole-body metabolism. *J Clin Invest*. 2011; 121:4222–4230. [PubMed: 22045572]
- Borg ML, Omran SF, Weir J, Meikle PJ, Watt MJ. Consumption of a high-fat diet, but not regular endurance exercise training, regulates hypothalamic lipid accumulation in mice. *J Physiol*. 2012; 590:4377–4389. [PubMed: 22674717]
- Cannon B, Nedergaard J. Brown adipose tissue: function and physiological significance. *Physiol Rev*. 2004; 84:277–359. [PubMed: 14715917]

- Car H, Zendzian-Piotrowska M, Prokopiuk S, Fiedorowicz A, Sadowska A, Kurek K, Sawicka D. Ceramide profiles in the brain of rats with diabetes induced by streptozotocin. *FEBS J.* 2012; 279:1943–1952. [PubMed: 22429392]
- Caro JF, Kolaczynski JW, Nyce MR, Ohannesian JP, Opentanova I, Goldman WH, Lynn RB, Zhang PL, Sinha MK, Considine RV. Decreased cerebrospinal-fluid/serum leptin ratio in obesity: a possible mechanism for leptin resistance. *Lancet.* 1996; 348:159–161. [PubMed: 8684156]
- Chavez JA, Summers SA. A ceramide-centric view of insulin resistance. *Cell Metab.* 2012; 15:585–594. [PubMed: 22560211]
- Cnop M, Foufelle F, Velloso LA. Endoplasmic reticulum stress, obesity and diabetes. *Trends Mol Med.* 2012; 18:59–68. [PubMed: 21889406]
- Cowart LA. Sphingolipids: players in the pathology of metabolic disease. *Trends Endocrinol Metab.* 2009; 20:34–42. [PubMed: 19008117]
- Dietrich MO, Horvath TL. Limitations in anti-obesity drug development: the critical role of hunger-promoting neurons. *Nat Rev Drug Discov.* 2012; 11:675–691. [PubMed: 22858652]
- Finan B, Yang B, Ottaway N, Stemmer K, Müller TD, Yi CX, Habegger K, Schriever SC, García-Cáceres C, Kabra DG, et al. Targeted estrogen delivery reverses the metabolic syndrome. *Nat Med.* 2012; 18:1847–1856. [PubMed: 23142820]
- Fu S, Watkins SM, Hotamisligil GS. The role of endoplasmic reticulum in hepatic lipid homeostasis and stress signaling. *Cell Metab.* 2012; 15:623–634. [PubMed: 22560215]
- Gao S, Zhu G, Gao X, Wu D, Carrasco P, Casals N, Hegardt FG, Moran TH, Lopaschuk GD. Important roles of brain-specific carnitine palmitoyltransferase and ceramide metabolism in leptin hypothalamic control of feeding. *Proc Natl Acad Sci USA.* 2011; 108:9691–9696. [PubMed: 21593415]
- Gregor MF, Hotamisligil GS. Inflammatory mechanisms in obesity. *Annu Rev Immunol.* 2011; 29:415–445. [PubMed: 21219177]
- Hannun YA, Obeid LM. Principles of bioactive lipid signalling: lessons from sphingolipids. *Nat Rev Mol Cell Biol.* 2008; 9:139–150. [PubMed: 18216770]
- Hendershot LM, Wei JY, Gaut JR, Lawson B, Freiden PJ, Murti KG. In vivo expression of mammalian BiP ATPase mutants causes disruption of the endoplasmic reticulum. *Mol Biol Cell.* 1995; 6:283–296. [PubMed: 7612964]
- Holland WL, Summers SA. Sphingolipids, insulin resistance, and metabolic disease: new insights from in vivo manipulation of sphingolipid metabolism. *Endocr Rev.* 2008; 29:381–402. [PubMed: 18451260]
- Holland WL, Brozinick JT, Wang LP, Hawkins ED, Sargent KM, Liu Y, Narra K, Hoehn KL, Knotts TA, Siesky A, et al. Inhibition of ceramide synthesis ameliorates glucocorticoid-, saturated-fat-, and obesity-induced insulin resistance. *Cell Metab.* 2007; 5:167–179. [PubMed: 17339025]
- Hosoi T, Sasaki M, Miyahara T, Hashimoto C, Matsuo S, Yoshii M, Ozawa K. Endoplasmic reticulum stress induces leptin resistance. *Mol Pharmacol.* 2008; 74:1610–1619. [PubMed: 18755873]
- Howard JK, Cave BJ, Oksanen LJ, Tzamelis I, Bjørbaek C, Flier JS. Enhanced leptin sensitivity and attenuation of diet-induced obesity in mice with haploinsufficiency of Socs3. *Nat Med.* 2004; 10:734–738. [PubMed: 15220914]
- Ilieva EV, Ayala V, Jové M, Dalfó E, Cacabelos D, Povedano M, Bellmunt MJ, Ferrer I, Pamplona R, Portero-Otín M. Oxidative and endoplasmic reticulum stress interplay in sporadic amyotrophic lateral sclerosis. *Brain.* 2007; 130:3111–3123. [PubMed: 17716997]
- Kahn SE, Hull RL, Utzschneider KM. Mechanisms linking obesity to insulin resistance and type 2 diabetes. *Nature.* 2006; 444:840–846. [PubMed: 17167471]
- Kammoun HL, Chabanon H, Hainault I, Luquet S, Magnan C, Koike T, Ferré P, Foufelle F. GRP78 expression inhibits insulin and ER stress-induced SREBP-1c activation and reduces hepatic steatosis in mice. *J Clin Invest.* 2009; 119:1201–1215. [PubMed: 19363290]
- Lam TK, Schwartz GJ, Rossetti L. Hypothalamic sensing of fatty acids. *Nat Neurosci.* 2005; 8:579–584. [PubMed: 15856066]
- Lipson KL, Fonseca SG, Ishigaki S, Nguyen LX, Foss E, Bortell R, Rossini AA, Urano F. Regulation of insulin biosynthesis in pancreatic beta cells by an endoplasmic reticulum-resident protein kinase IRE1. *Cell Metab.* 2006; 4:245–254. [PubMed: 16950141]

- López M, Lage R, Saha AK, Pérez-Tilve D, Vázquez MJ, Varela L, Sangiao-Alvarellos S, Tovar S, Raghay K, Rodríguez-Cuenca S, et al. Hypothalamic fatty acid metabolism mediates the orexigenic action of ghrelin. *Cell Metab.* 2008; 7:389–399. [PubMed: 18460330]
- López M, Varela L, Vázquez MJ, Rodríguez-Cuenca S, González CR, Velagapudi VR, Morgan DA, Schoenmakers E, Agassandian K, Lage R, et al. Hypothalamic AMPK and fatty acid metabolism mediate thyroid regulation of energy balance. *Nat Med.* 2010; 16:1001–1008. [PubMed: 20802499]
- López M, Alvarez CV, Nogueiras R, Diéguez C. Energy balance regulation by thyroid hormones at central level. *Trends Mol Med.* 2013; 19:418–427. [PubMed: 23707189]
- Luquet S, Magnan C. The central nervous system at the core of the regulation of energy homeostasis. *Front Biosci (Schol Ed).* 2009; 1:448–465. [PubMed: 19482713]
- Malik VS, Willett WC, Hu FB. Global obesity: trends, risk factors and policy implications. *Nat Rev Endocrinol.* 2013; 9:13–27. [PubMed: 23165161]
- Marciniak SJ, Ron D. Endoplasmic reticulum stress signaling in disease. *Physiol Rev.* 2006; 86:1133–1149. [PubMed: 17015486]
- Martínez de Morentin PB, López M. “Mens sana in corpore sano”: exercise and hypothalamic ER stress. *PLoS Biol.* 2010; 8:e1000464. [PubMed: 20808779]
- Martínez de Morentin PB, Varela L, Fernø J, Nogueiras R, Diéguez C, López M. Hypothalamic lipotoxicity and the metabolic syndrome. *Biochim Biophys Acta.* 2010; 1801:350–361. [PubMed: 19796707]
- Martínez de Morentin PB, Whittle AJ, Fernø J, Nogueiras R, Diéguez C, Vidal-Puig A, López M. Nicotine induces negative energy balance through hypothalamic AMP-activated protein kinase. *Diabetes.* 2012; 61:807–817. [PubMed: 22315316]
- Martínez de Morentin PB, González-García I, Martins L, Lage R, Fernández-Mallo D, Martínez-Sánchez N, Ruíz-Pino F, Liu J, Morgan DA, Pinilla L, et al. Estradiol regulates brown adipose tissue thermogenesis via hypothalamic AMPK. *Cell Metab.* 2014; 20:41–53. [PubMed: 24856932]
- McCrimmon RJ, Fan X, Cheng H, McNay E, Chan O, Shaw M, Ding Y, Zhu W, Sherwin RS. Activation of AMP-activated protein kinase within the ventromedial hypothalamus amplifies counterregulatory hormone responses in rats with defective counterregulation. *Diabetes.* 2006; 55:1755–1760. [PubMed: 16731839]
- McCrimmon RJ, Shaw M, Fan X, Cheng H, Ding Y, Vella MC, Zhou L, McNay EC, Sherwin RS. Key role for AMP-activated protein kinase in the ventromedial hypothalamus in regulating counterregulatory hormone responses to acute hypoglycemia. *Diabetes.* 2008; 57:444–450. [PubMed: 17977955]
- Mitoma J, Ito M, Furuya S, Hirabayashi Y. Bipotential roles of ceramide in the growth of hippocampal neurons: promotion of cell survival and dendritic outgrowth in dose- and developmental stage-dependent manners. *J Neurosci Res.* 1998; 51:712–722. [PubMed: 9545085]
- Ozcan U, Cao Q, Yilmaz E, Lee AH, Iwakoshi NN, Ozdelen E, Tuncman G, Görgün C, Glimcher LH, Hotamisligil GS. Endoplasmic reticulum stress links obesity, insulin action, and type 2 diabetes. *Science.* 2004; 306:457–461. [PubMed: 15486293]
- Ozcan U, Yilmaz E, Ozcan L, Furuhashi M, Vaillancourt E, Smith RO, Görgün CZ, Hotamisligil GS. Chemical chaperones reduce ER stress and restore glucose homeostasis in a mouse model of type 2 diabetes. *Science.* 2006; 313:1137–1140. [PubMed: 16931765]
- Ozcan L, Ergin AS, Lu A, Chung J, Sarkar S, Nie D, Myers MG Jr, Ozcan U. Endoplasmic reticulum stress plays a central role in development of leptin resistance. *Cell Metab.* 2009; 9:35–51. [PubMed: 19117545]
- Phillips MS, Liu Q, Hammond HA, Dugan V, Hey PJ, Caskey CJ, Hess JF. Leptin receptor missense mutation in the fatty Zucker rat. *Nat Genet.* 1996; 13:18–19. [PubMed: 8673096]
- Picard A, Rouch C, Kassis N, Moullé VS, Croizier S, Denis RG, Castel J, Coant N, Davis K, Clegg DJ, et al. Hippocampal lipoprotein lipase regulates energy balance in rodents. *Mol Metab.* 2014; 3:167–176. [PubMed: 24634821]
- Ramachandrapa S, Farooqi IS. Genetic approaches to understanding human obesity. *J Clin Invest.* 2011; 121:2080–2086. [PubMed: 21633175]

- Ramírez S, Martíns L, Jacas J, Carrasco P, Pozo M, Clotet J, Serra D, Hegardt FG, Diéguez C, López M, Casals N. Hypothalamic ceramide levels regulated by CPT1C mediate the orexigenic effect of ghrelin. *Diabetes*. 2013; 62:2329–2337. [PubMed: 23493572]
- Ron D, Walter P. Signal integration in the endoplasmic reticulum unfolded protein response. *Nat Rev Mol Cell Biol*. 2007; 8:519–529. [PubMed: 17565364]
- Ropelle ER, Flores MB, Cintra DE, Rocha GZ, Pauli JR, Morari J, de Souza CT, Moraes JC, Prada PO, Guadagnini D, et al. IL-6 and IL-10 anti-inflammatory activity links exercise to hypothalamic insulin and leptin sensitivity through IKKbeta and ER stress inhibition. *PLoS Biol*. 2010; 8:e1000465. [PubMed: 20808781]
- Schneeberger M, Dietrich MO, Sebastián D, Imbernón M, Castaño C, Garcia A, Esteban Y, Gonzalez-Franquesa A, Rodríguez IC, Bortolozzi A, et al. Mitofusin 2 in POMC neurons connects ER stress with leptin resistance and energy imbalance. *Cell*. 2013; 155:172–187. [PubMed: 24074867]
- Schröder M, Kaufman RJ. The mammalian unfolded protein response. *Annu Rev Biochem*. 2005; 74:739–789. [PubMed: 15952902]
- Seoane-Collazo P, Martínez de Morentin PB, Fernø J, Diéguez C, Nogueiras R, López M. Nicotine improves obesity and hepatic steatosis and ER stress in diet-induced obese male rats. *Endocrinology*. 2014; 155:1679–1689. [PubMed: 24517227]
- Shen J, Chen X, Hendershot L, Prywes R. ER stress regulation of ATF6 localization by dissociation of BiP/GRP78 binding and unmasking of Golgi localization signals. *Dev Cell*. 2002; 3:99–111. [PubMed: 12110171]
- Speakman JR, O’Rahilly S. Fat: an evolving issue. *Dis Model Mech*. 2012; 5:569–573. [PubMed: 22915015]
- Summers SA, Garza LA, Zhou H, Birnbaum MJ. Regulation of insulin-stimulated glucose transporter GLUT4 translocation and Akt kinase activity by ceramide. *Mol Cell Biol*. 1998; 18:5457–5464. [PubMed: 9710629]
- Symons JD, Abel ED. Lipotoxicity contributes to endothelial dysfunction: a focus on the contribution from ceramide. *Rev Endocr Metab Disord*. 2013; 14:59–68. [PubMed: 23292334]
- Unger RH. Lipotoxic diseases. *Annu Rev Med*. 2002; 53:319–336. [PubMed: 11818477]
- Virtue S, Vidal-Puig A. It’s not how fat you are, it’s what you do with it that counts. *PLoS Biol*. 2008; 6:e237. [PubMed: 18816166]
- Virtue S, Vidal-Puig A. Adipose tissue expandability, lipotoxicity and the Metabolic Syndrome—an allostatic perspective. *Biochim Biophys Acta*. 2010; 1801:338–349. [PubMed: 20056169]
- Whittle AJ, Carobbio S, Martíns L, Slawik M, Hondares E, Vázquez MJ, Morgan D, Csikasz RI, Gallego R, Rodriguez-Cuenca S, et al. BMP8B increases brown adipose tissue thermogenesis through both central and peripheral actions. *Cell*. 2012; 149:871–885. [PubMed: 22579288]
- Williams KW, Elmquist JK. From neuroanatomy to behavior: central integration of peripheral signals regulating feeding behavior. *Nat Neurosci*. 2012; 15:1350–1355. [PubMed: 23007190]
- Won JC, Jang PG, Namkoong C, Koh EH, Kim SK, Park JY, Lee KU, Kim MS. Central administration of an endoplasmic reticulum stress inducer inhibits the anorexigenic effects of leptin and insulin. *Obesity (Silver Spring)*. 2009; 17:1861–1865. [PubMed: 19543218]
- Yang G, Badeanlou L, Bielawski J, Roberts AJ, Hannun YA, Sa-mad F. Central role of ceramide biosynthesis in body weight regulation, energy metabolism, and the metabolic syndrome. *Am J Physiol Endocrinol Metab*. 2009; 297:E211–E224. [PubMed: 19435851]
- Yeo GS, Heisler LK. Unraveling the brain regulation of appetite: lessons from genetics. *Nat Neurosci*. 2012; 15:1343–1349. [PubMed: 23007189]
- Zhang X, Zhang G, Zhang H, Karin M, Bai H, Cai D. Hypothalamic IKKbeta/NF-kappaB and ER stress link overnutrition to energy imbalance and obesity. *Cell*. 2008; 135:61–73. [PubMed: 18854155]

Highlights

Ceramides induce hypothalamic lipotoxicity and ER stress, leading to weight gain

The chaperone GRP78/BiP in the hypothalamus abolishes ceramide action

Genetic inhibition of hypothalamic GRP78 induces weight gain

Obese Zucker rats show elevated hypothalamic ceramides and ER stress

Author Manuscript

Author Manuscript

Author Manuscript

Author Manuscript

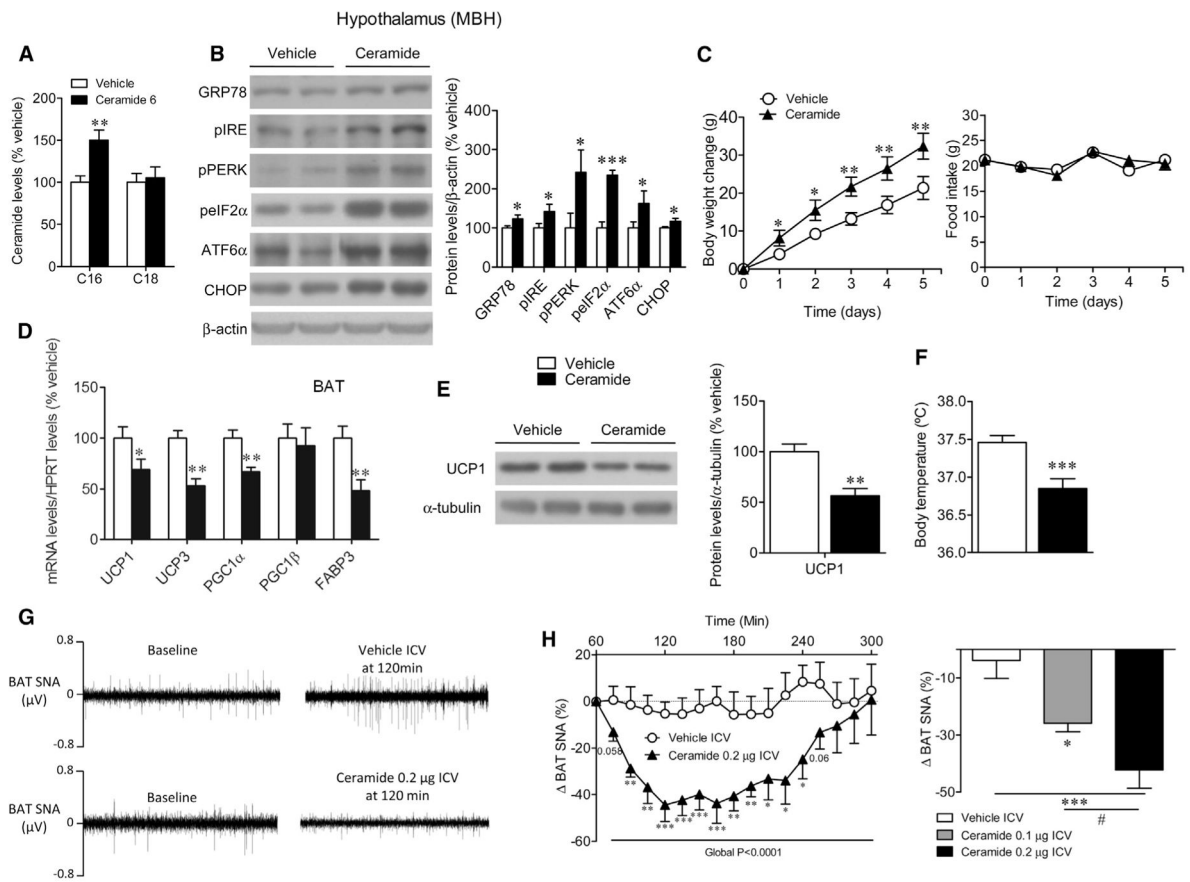


Figure 1. Effect of Central Administration of Ceramide on Energy Balance

Ceramide levels in the mediobasal hypothalamus (MBH) (A), representative western blot autoradiographic images (B, left; spliced bands loaded in the same gel) and hypothalamic protein levels of UPR (B, right), body weight change (C, left) and daily food intake (C, right), mRNA expression in the BAT (D), representative western blot autoradiographic images (E, left; spliced bands loaded in the same gel) and protein levels of BAT UCP1 (E, right), rectal temperature (F), BAT sympathetic nervous activity (SNA) tracings (G), and change in BAT SNA of rats centrally treated with vehicle or ceramide 6 (H). Error bars represent SEM; n = 5–7 (SNA recordings) or n = 7–26 animals per experimental group. *p < 0.05, **p < 0.01, and ***p < 0.001 versus vehicle, #p < 0.05 ceramide 0.2 μg ICV versus ceramide 0.1 μg ICV.

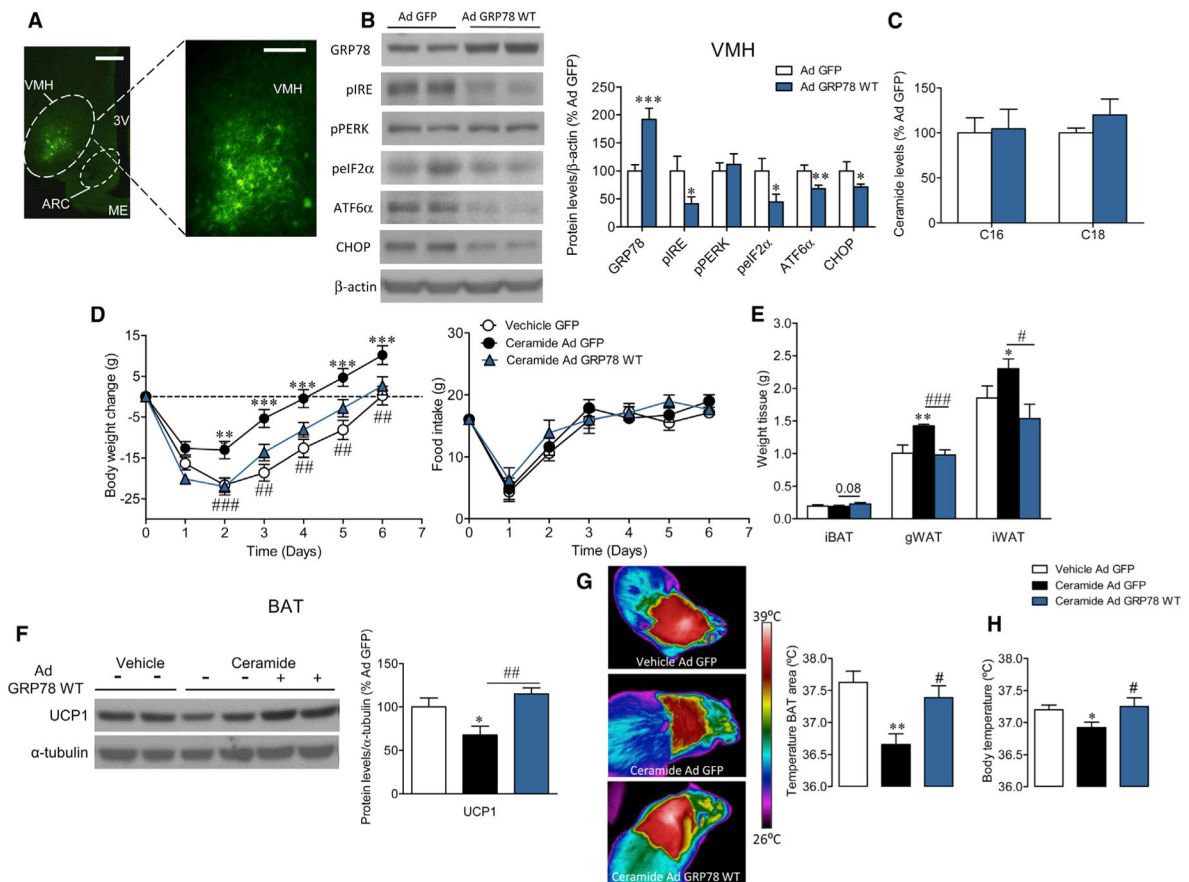


Figure 2. Effect of GRP78 Overexpression in the VMH on Central Ceramide Actions and Energy Balance

(A–C) Representative immunofluorescence (A, left: 4×, scale bar, 300 μm; A, right: 20×, scale bar 100 μm) with anti-GFP showing GFP expression in the VMH, representative western blot autoradiographic images (B, left; spliced bands loaded in the same gel) and hypothalamic protein levels of UPR (B, right; see Figure S1A for analysis of inflammatory markers in the hypothalamus), and ceramide levels (C) in the mediobasal hypothalamus of rats treated with GFP or GRP78 WT adenoviruses into the VMH.

(D–H) Body weight change (D, left) and daily food intake (D, right); weight of iBAT, gWAT, and iWAT pads (E); representative western blot autoradiographic images (F, left; spliced bands loaded in the same gel) and protein levels of BAT UCP1 (F, right); representative infrared thermal images (G, left) and temperature of the BAT area (G, right); and rectal temperature (H) of rats centrally treated with vehicle or ceramide and stereotaxically treated with GFP or GRP78 WT adenoviruses into the VMH. In order to simplify (D)–(H), the vehicle Ad GRP78 WT group has been omitted; in any case, it is important to note that no differences were found in that group when compared to vehicle Ad GFP (see Figures S1B and S1C).

Error bars represent SEM; n = 6 (fat pads and temperature) or 7–47 animals per experimental group. 3V, third ventricle; ME, median eminence. *p < 0.05, ** p < 0.01, and ***p < 0.001 versus Ad GFP or vehicle Ad GFP; #p < 0.05, ## p < 0.01, and ###p < 0.001

ceramide Ad GFP versus ceramide Ad GRP78 WT. See Figures S1D–S1H for analysis of GRP78 WT adenoviruses in the arcuate nucleus of the hypothalamus.

Author Manuscript

Author Manuscript

Author Manuscript

Author Manuscript

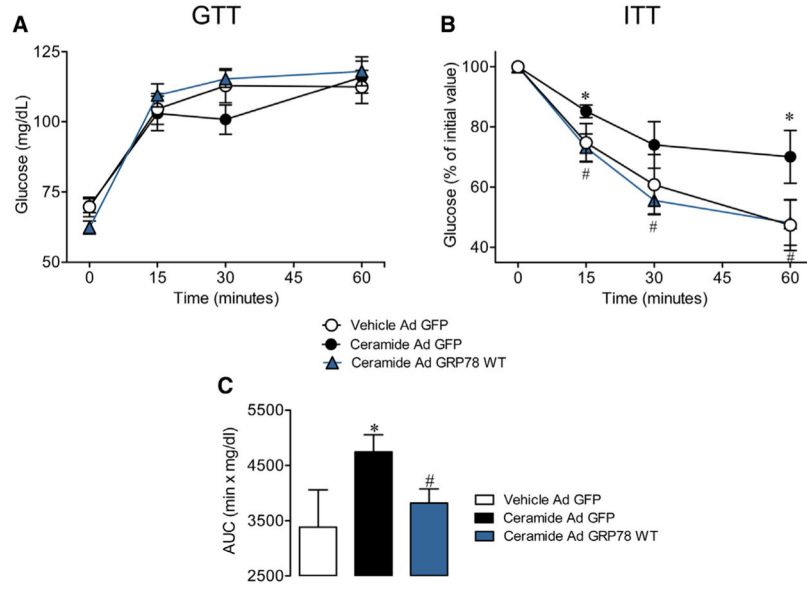


Figure 3. Effect of GRP78 Overexpression in the VMH on Central Ceramide Actions on Glucose Homeostasis and Insulin Sensitivity

Glucose tolerance test (GTT) (A), insulin tolerance test (ITT) (B), and area under the curve (AUC) (C) from ITT of rats centrally treated with vehicle or ceramide and stereotactically treated with GFP or GRP78 WT adenoviruses into the VMH. Error bars represent SEM; n = 7–9 animals per experimental group. *p < 0.05 versus vehicle Ad GFP; # p < 0.05 ceramide Ad GFP versus ceramide Ad GRP78 WT.

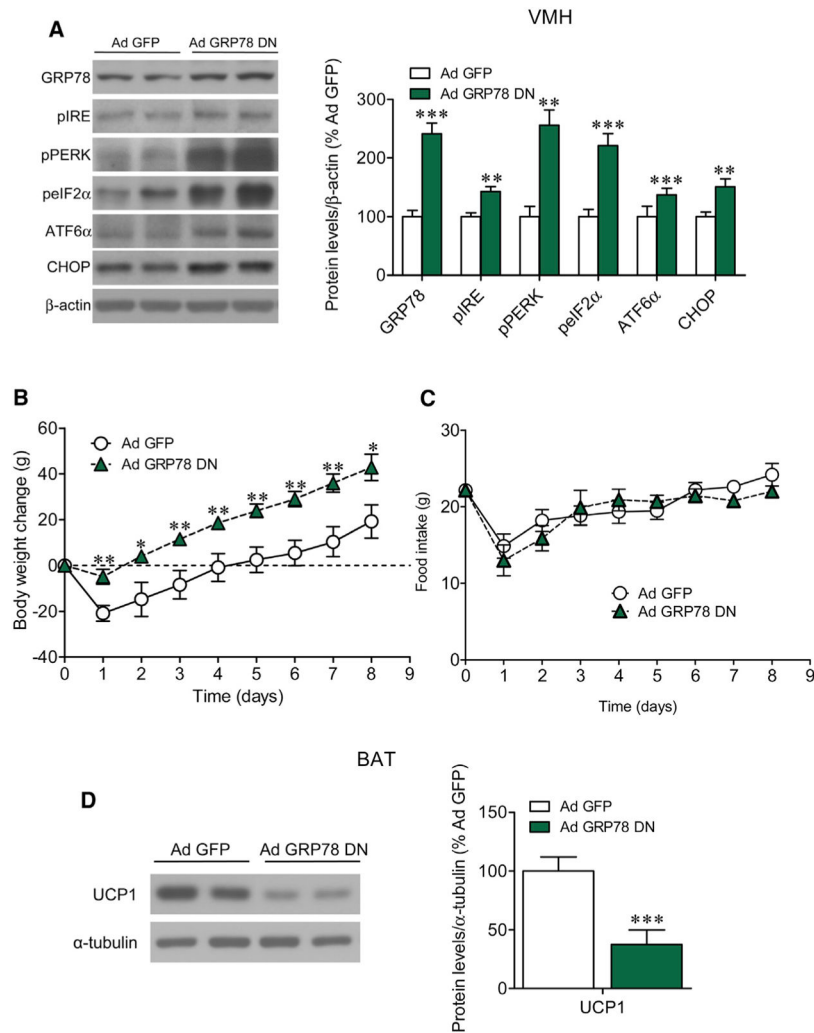


Figure 4. Effect of GRP78 Inhibition in the VMH on Energy Balance

Representative western blot autoradiographic images (A, left; spliced bands loaded in the same gel) and hypothalamic protein levels of UPR (A, right), body weight change (B), daily food intake (C), and representative western blot autoradiographic images (D, left; spliced bands loaded in the same gel) and protein levels of BAT UCP1 (D, right) of rats treated with GFP or GRP78 DN adenoviruses into the VMH. Error bars represent SEM; n = 7–9 animals per experimental group. *p < 0.05, ** p < 0.01, and ***p < 0.001 versus Ad GFP. See Figure S2 for analysis of GRP78 DN adenoviruses in the arcuate nucleus of the hypothalamus.

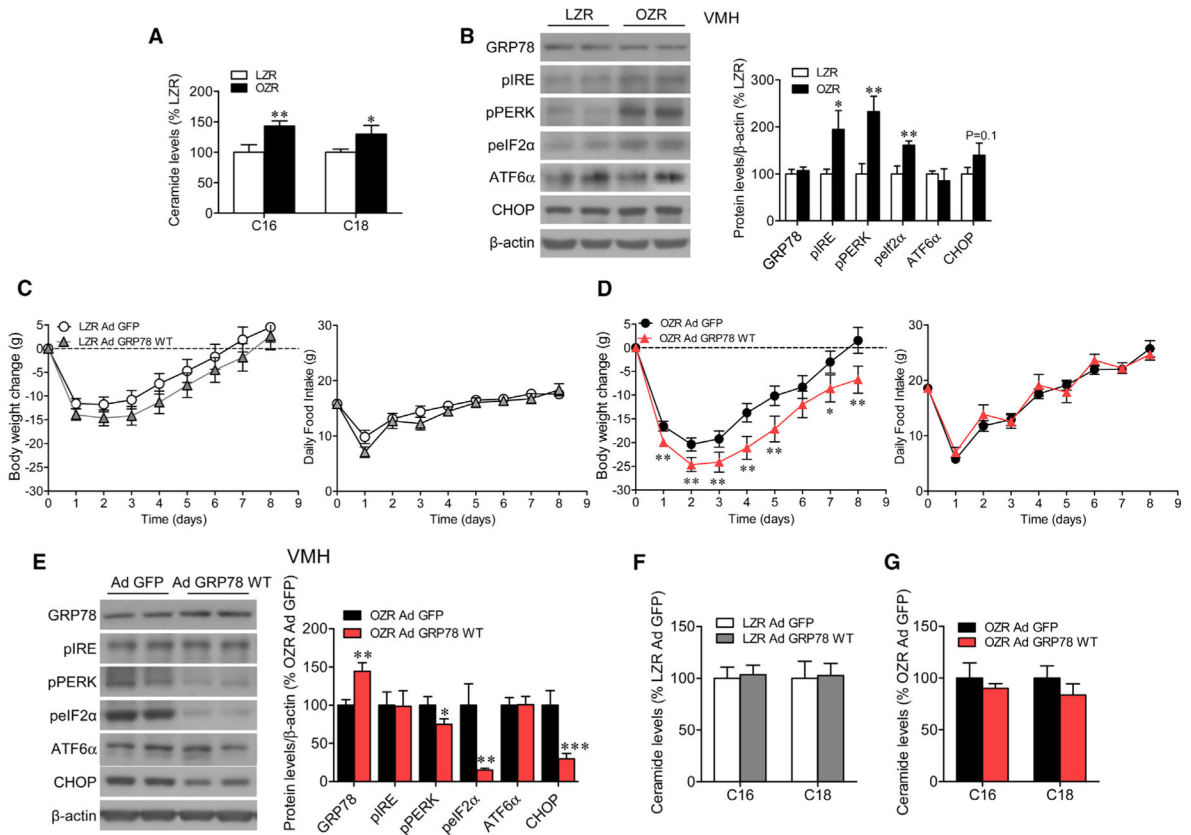


Figure 5. Effect of GRP78 Overexpression in the VMH of Obese Zucker Rats on Energy Balance (A and B) Ceramide levels in the mediobasal hypothalamus (A) and representative western blot autoradiographic images (B, left; spliced bands loaded in the same gel) and hypothalamic protein levels of UPR (B, right) in LZR and OZR. (C–G) Body weight change (C and D, left) and daily food intake (C and D, right) from LZR and OZR, respectively; representative western blot autoradiographic images (E, left; spliced bands loaded in the same gel) and VMH protein levels of UPR from OZR (E, right); and ceramide levels in the mediobasal hypothalamus of LZR (F) and OZR (G) stereotactically treated with GFP or GRP78 WT adenoviruses into the VMH. Error bars represent SEM; n = 7–33 animals per experimental group. *p < 0.05, **p < 0.01, ***p < 0.001 versus LZR or OZR Ad GFP.

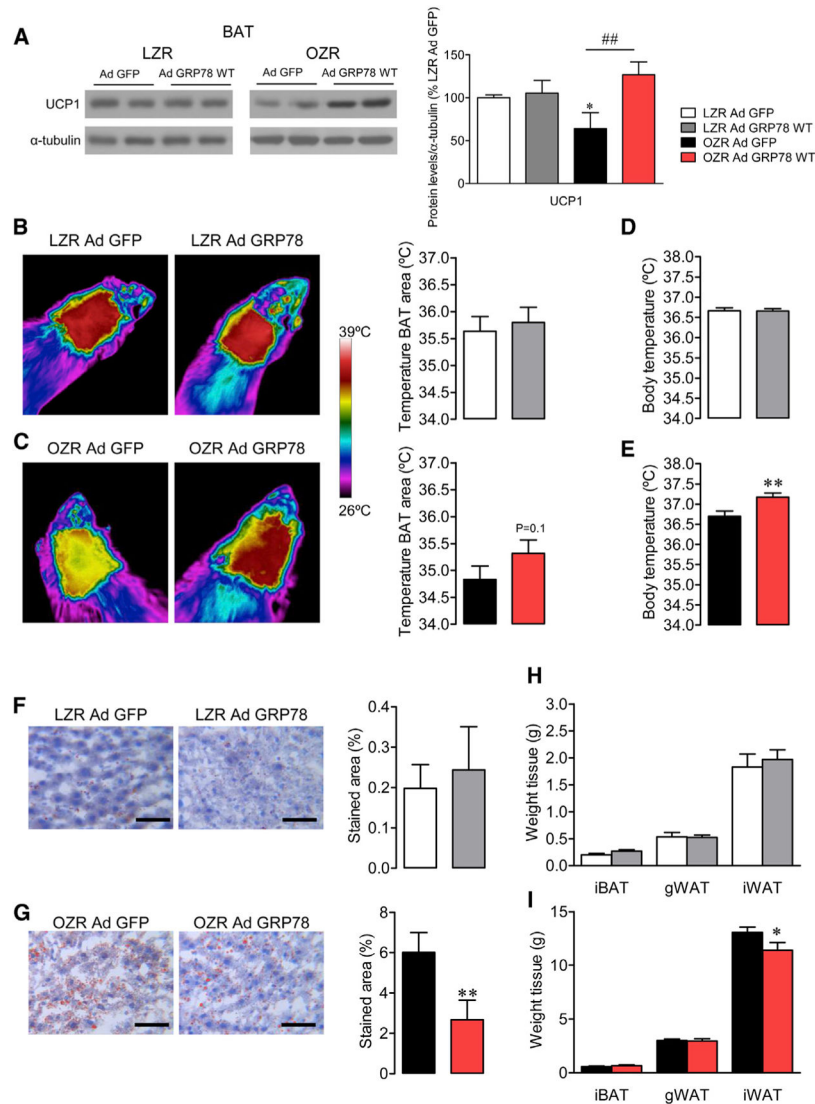


Figure 6. Effect of GRP78 Overexpression in the VMH of Obese Zucker Rats on BAT Thermogenesis and Liver Steatosis

Representative western blot autoradiographic images (A, left; spliced bands loaded in the same gel) and protein levels of BAT UCP1 (A, right); representative infrared thermal images (B and C, left) and temperature of the BAT area (B and C, right); rectal temperature (D and E); representative oil red O-stained liver sections (F and G, left; scale bar, 50 μ m) and their quantification (F and G, right panel); and weight of iBAT, gWAT, and iWAT pads from LZR (H) and OZR (I) stereotaxically treated with GFP or GRP78 WT adenoviruses into the VMH. Error bars represent SEM; n = 7–9 animals per experimental group. *p < 0.05 and **p < 0.01 versus LZR or OZR Ad GFP; ##p < 0.01 OZR Ad GFP versus OZR Ad GRP78 WT.

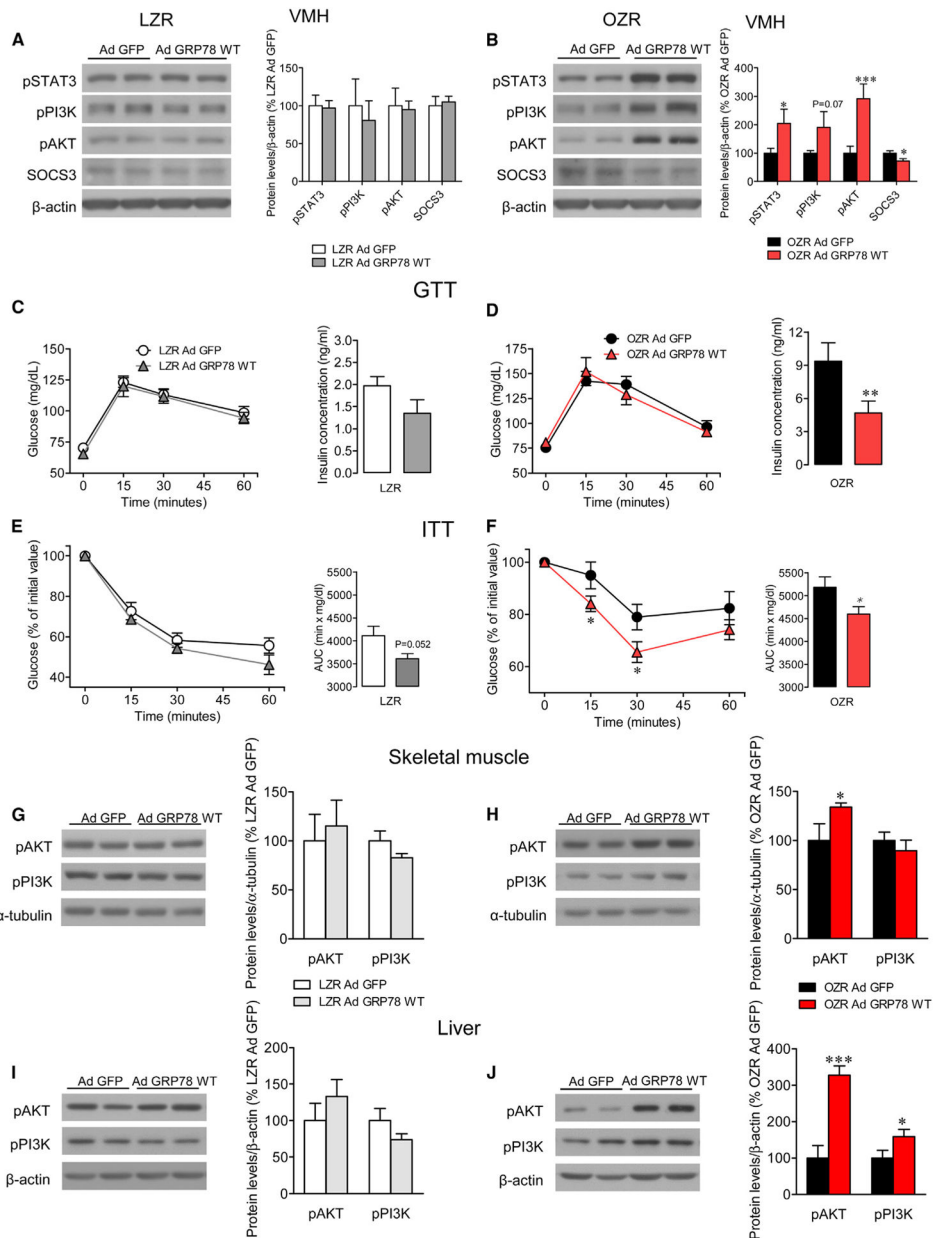


Figure 7. Effect of GRP78 Overexpression in the VMH of Obese Zucker Rats on Leptin Signaling, Glucose Homeostasis, and Insulin Sensitivity

Representative western blot autoradiographic images (A and B, left; spliced bands loaded in the same gel) and hypothalamic protein levels of leptin signaling pathway in the VMH (A and B, right) from LZR and OZR; GTT (C and D, left) and serum insulin concentration after 30 min of glucose administration (C and D, right); ITT (E and F, left) and area under the curve (AUC) from ITT (E and F, right); and representative western blot autoradiographic images (G–J, left; spliced bands loaded in the same gel) and protein levels of insulin signaling pathway in skeletal muscle and liver (G–J, right) of LZR and OZR stereotactically treated with GFP or GRP78 WT adenoviruses into the VMH. Error bars represent SEM; n =

6 (pAKT and pPI3K in LZR) or $n = 7-10$ animals per experimental group. $*p < 0.05$, $**p < 0.01$, and $***p < 0.001$ versus LZR Ad GFP or OZR Ad GFP.

Author Manuscript

Author Manuscript

Author Manuscript

Author Manuscript